Available online at www.sciencedirect.com

ScienceDirect

Ceramics International 40 (2014) 423–427

CERAMICS INTERNATIONAL

www.elsevier.com/locate/ceramint

Synthesis of High aspect ratio $CdTiO_3$ nanofibers via electrospinning: characterization and photocatalytic activity

M. Shamshi Hassan[a,*], Touseef Amna[b], Myung-Seob Khil[a,*]

[a]Department of organic materials and fiber Engineering, Chonbuk National University, Jeonju 561-756, Republic of Korea
[b]Department of Animal Science and Biotechnology, Chonbuk National University, Jeonju 561-756, Republic of Korea

Received 2 May 2013; received in revised form 5 June 2013; accepted 10 June 2013
Available online 18 June 2013

Abstract

We for the first time report $CdTiO_3$ nanofibers as an effective photocatalyst for the photodegradation of Rhodamine 6G (R6G) dye. One-dimensional $CdTiO_3$ nanofibers with high aspect ratio have been successfully synthesized by the sol–gel electrospinning technique. X-ray diffraction (XRD), Field emission scanning electron microscopy (FE-SEM), transmission electron microscopy (TEM), energy-dispersive X-ray (EDX) spectroscopy, thermogravimetric analysis (TGA), UV–vis diffuse reflectance (DR) and Raman spectroscopy were used to characterize the synthesized nanofibers. The photocatalytic activity of the electrospun $CdTiO_3$ was evaluated by performing photodegradation of R6G dye under UV light irradiation. Our results indicated that the $CdTiO_3$ fibers were in nanometer scale with diameters ranging from of 350–400 nm which consisted of rhombohedral structure. The superior photocatalytic activity of the $CdTiO_3$ nanofibers calcined at 800 °C for the degradation of R6G dye could be attributed to the high degree of crystallinity and absorption properties of the samples synthesized at high temperature. This study indicates the potential use of high aspect ratio $CdTiO_3$ nanofibers for removal of industrial pollutants and noxious wastes.

Keywords: $CdTiO_3$; Electrospinning; Nanofibers; Dye degradation

1. Introduction

With the ever-increasing use of a wide variety of dyes in textile, photography, coatings and so on, pollution of water by these dyes has become increasingly alarming. Color removal, in particular, has recently become a major scientific concern. Wastewaters from various sources such as industries, factories, laboratories, etc. are serious problems to the environment. The discharged wastes containing dyes are toxic to micro-organisms, aquatic life and human beings [1]. These deleterious chemicals severely disturb the aquatic ecosystem or/the earth's ecosystems. The degradation of dyes in industrial wastewaters has therefore received increasing attention and for this purpose some methods of remediation have been preferred. To this end, photocatalysis using nanotextured semiconductor materials has turned out to be a promising alternative for management of the water environment [2,3]. The nanostructured semiconductors have great potential in the removal of dyes from wastewaters due to their unique ability to completely mineralize the target pollutants [4]. It has been reported that TiO_2 [5], Zn_2SnO_4 [6], $BiVO_4$ [7], Bi_2MoO_6 [8] and $CdWO_4$ [9] shows excellent photocatalytic activity under ultraviolet or visible light irradiation. Among the various semiconductors, the perovskite has been regarded as a promising photocatalyst, since it presents more activity in long bands of visible light.

Titanium-based oxides with perovskite crystalline phase have been widely studied because of their diverse applications. Cadmium titanate is one of the members of smart family which shows excellent dielectric, piezoelectric, pyroelectric and photostrictive properties [10]. Cadmium titanate has also been used as a conductive material [11,12], optical fibers [13], humidity sensing [14], and photocatalytic [15]. Several methods have been reported for the synthesis of cadmium titanate like sol–gel [16,17], solid state method [18], hydrothermal method [19] etc. Nevertheless, the electrospinning is known as a simple and versatile method for generating

---

*Corresponding authors. Tel.: +82 63 270 4635; fax: +82 63 270 23.
E-mail addresses: shamshi@jbnu.ac.kr (M. Shamshi Hassan), mskhil@jbnu.ac.kr (M.-S. Khil).

0272-8842/$ - see front matter © 2013 Elsevier Ltd and Techna Group S.r.l. All rights reserved.
http://dx.doi.org/10.1016/j.ceramint.2013.06.018

nanofibers. Nowadays, this technique has extended to the fabrication of ceramic and composite nanofibers with various compositions and properties. Nanofibers are of great importance for applications in photocatalysis, supercapacitors, sensing, actuators, solar and fuel cells. Particularly, one dimensional porous titania nanofibers consisting of well crystallized anatase nanocrystals are very advantageous for developing active photocatalytic materials for environmental purification and green energy [20]. Such materials are usually having a large surface area and high porosity. A larger surface area provides more surface active sites for the adsorption of reactant molecules, which thus make the photocatalytic process more efficient [21]. Furthermore, the electrospun nanofibers have large surface area and regular morphology on the nanometer scale.

Considering the novel properties of titania and cadmium; the present study was aimed to fabricate the $CdTiO_3$ nanofibers by the electrospinning method and the characterization of synthesized nanofibers was done by sophisticated techniques such as XRD, FE-SEM, HR-TEM, EDX and UV–vis spectra. To the best of our knowledge, there is no report about the photocatalytic activity of $CdTiO_3$ nanofibers. To this end, for the first time we investigated the degradation of R6G dye by $CdTiO_3$ nanofibers under UV light. Moreover, it was also established that the $CdTiO_3$ nanofibers calcined at 800 °C considerably degrade the R6G dye, thus indicates the potential use of synthesized nanofibers for removal of pollutants and noxious wastes.

2. Experimental

2.1. Materials and methods

Poly(vinyl acetate) (PVAc, Mw = 500,000) and cadmium acetate dihydrate, ($Cd(CH_3COO)_2 \cdot 2H_2O$) were purchased from Sigma-Aldrich, USA. *N*,*N*-dimethylformamide (DMF) and titanium isopropoxide (TIP, 98.0 assay), were obtained from Showa Co. and Junsei Co., Japan respectively.

2.2. Synthesis of $CdTiO_3$ nanofibers

In a typical procedure, PVAc (18 wt%) solution was prepared by dissolving PVAc in DMF under magnetic stirring for 6 h at room temperature. 1 mol of TIP was taken in a separate bottle and a few drops of acetic acid were added till the solution turned out to be transparent. Equimolar concentration of $Cd(NO_3)_2 \cdot 6H_2O$ (4 ml) was dissolved in ethanol and added into the TIP solution. The solution of cadmium acetate and TIP was mixed together. The final solution was made by mixing this solution with the PVAc solution in the ratio of 1:3. The obtained sol–gel was transferred into a 10 ml syringe with a stainless steel needle. A copper pin connected to a high voltage generator was inserted in the solution as a positive terminal, whereas a ground iron drum covered by a polyethylene sheet served as counter electrode. The solution was kept in the capillary by adjusting the inclination angle. A voltage of 15 kV was applied to this solution. The distance between the tip of the needle and collector was fixed at 18 cm. The as-spun composite nanofibers were initially dried at 80 °C for 24 h under vacuum. In order to remove the polymer, the composite samples were calcined at 600 and 800 °C in air with heating rate of 2 °C/min for 2 h.

2.3. Characterization

The XRD pattern of synthesized product was recorded on a Rigaku/Max-3 A X-ray diffractometer (XRD, Rigaku Co., Japan) with Cu Kα radiation ($\lambda = 1.540$ Å) over Bragg angles ranging from 20° to 80° and the operating voltage and current were maintained at 30 kV and 40 mA respectively. To examine the microstructure, the powder sample was uniformly sprayed on carbon tape, Pt coating was applied for 10 s onto the synthesized nanofibers and images were acquired at various magnifications via FE-SEM (JSM6700, JEOL, Japan). The diameters of the e-spun nanofibers were measured directly from the SEM images. Atleast 20 measurements for each sample were analyzed to obtain an average value. The chemical composition of the nanofibers was analyzed by EDX and the microscopic features of composite nanofibers were examined by TEM (H-7650, Hitachi, Japan). The thermal stability of the samples was characterized by thermogravimetric analysis (TGA-DTA, Perkin-Elmer Inc., USA) under air with a flow rate of 20 ml/min. The samples (~2–5 mg) were heated in a platinum pan from 25 °C to 800 °C at scanning rates of 10 °C/min. The light absorbance of the samples was measured by using a UV–vis diffused reflectance spectrum (UV-DRS, 525 Shimadzu).

The photocatalytic degradation was carried out by mixing 100 mg of the $CdTiO_3$ photocatalysts into the 100 ml of (10 ppm) R6G aqueous solution under continuous stirring. The experiments were performed at room temperature and prior to irradiation, the slurry was aerated for 30 min to reach adsorption equilibrium followed by UV irradiation. Aliquots were withdrawn from the suspension at specific time intervals and centrifuged immediately at 12000 rpm. The absorbance of the R6G solution was measured with a UV–vis spectrophotometer (Shimadzu UV-3101).

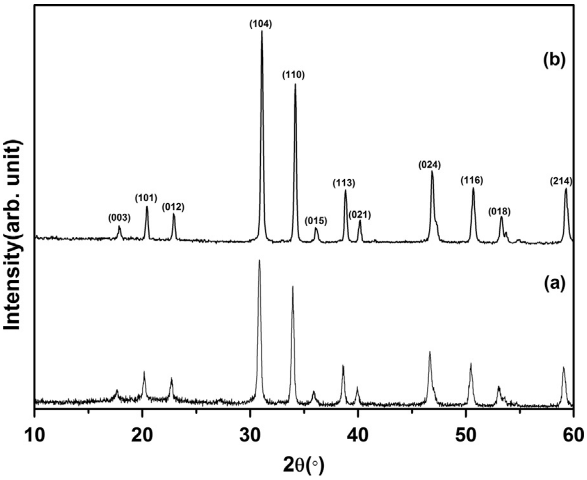

Fig. 1. XRD pattern of $CdTiO_3$ nanofibers at (a) 600 °C and (b) 800 °C.

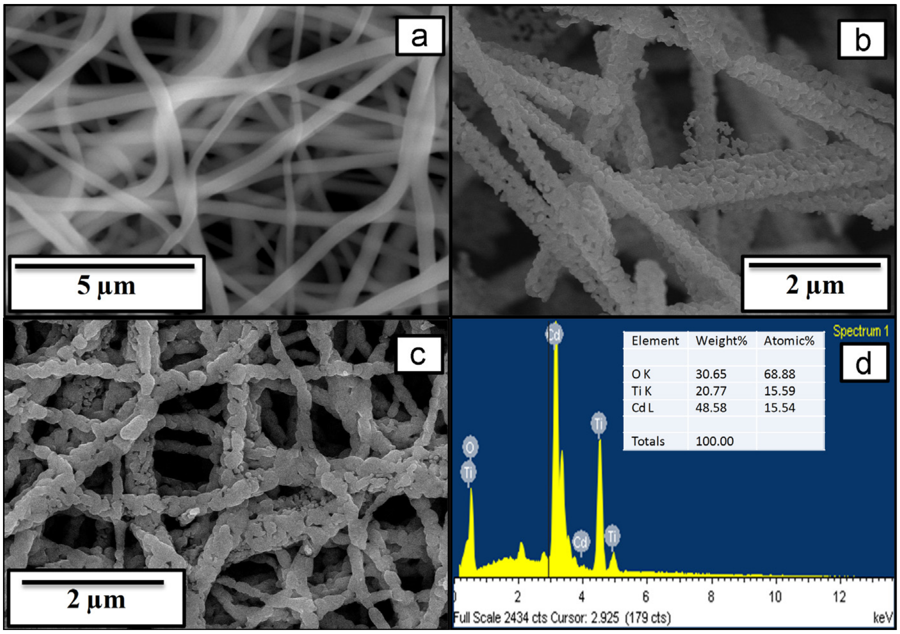

Fig. 2. SEM micrographs (a) as synthesized (b) at 600 °C (c) 800 °C and (d) EDX spectra of $CdTiO_3$ nanofibers.

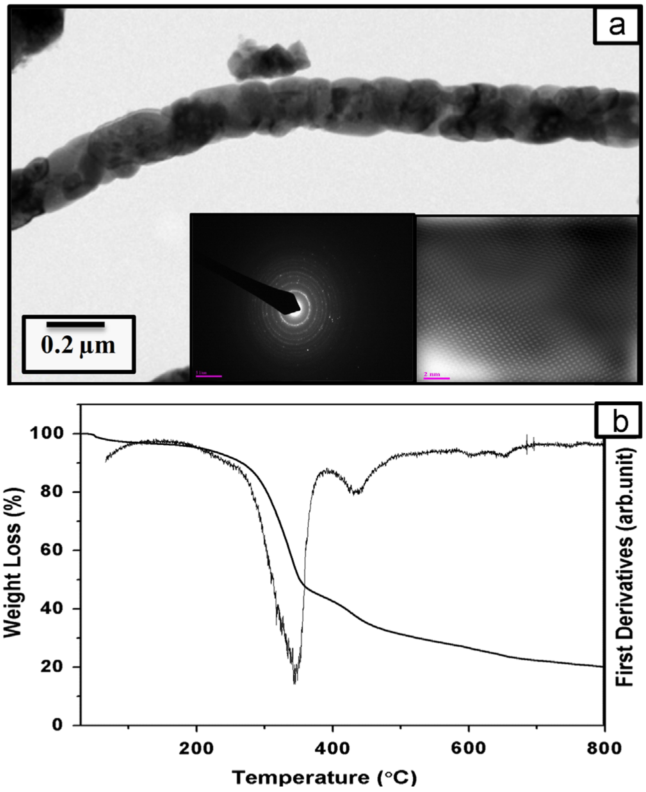

Fig. 3. (a) TEM micrographs of $CdTiO_3$ nanofibers. The inset in (a) shows the SAED pattern and corresponding FFT pattern. (b) Thermal gravimetric analysis in an air atmosphere and the corresponding first derivative of $CdTiO_3$ nanofibers.

3. Results and discussion

The XRD pattern of electrospun $CdTiO_3$ nanofibers calcined at different temperatures were shown in Fig. 1. Both the diffraction peaks in Fig. 1a and b could be perfectly indexed as rhombohedral structure (JCPDS 29–0277) [18]. The diffraction peaks of $CdTiO_3$ nanofibers calcined at 800 °C were sharp and intense, indicating high crystallinity of the nanofibers (Fig. 1b). No impurity peaks were observed in the spectra of both the samples, suggesting that the composition of the above nanofibers was $CdTiO_3$. By applying the Debye-Scherrer formula the average grain sizes of the products were calculated. The average grain size of the sample calcined at the 800 °C (62.7 nm) which is larger than that of the sample calcined at the 600 °C (53.7 nm).

Fig. 2a, b and c showed the typical SEM images of the electrospun nanofibers. From Fig. 2a, the as-spun sample showed randomly oriented nanofibers with smooth and uniform surface due to the amorphous nature of the $PVAc/Cd(NO_3)_2 \cdot 6H_2O/TiP$ composite nanofibers. Their lengths could reach several micrometers and the diameter of the above composite nanofibers ranged from 425 nm to 450 nm. As shown in Fig. 2b, c, the $CdTiO_3$ nanofibers, which were obtained by heat treatment of the above $PVAc/\ Cd(NO_3)_2 \cdot 6\,H_2O/TiP$ composite nanofibers, exhibited shrinkage resulting from the decomposition of PVAc. The diameter of $CdTiO_3$ nanofibers calcined at 600 °C ($\sim 390 \pm 10$ nm) (Fig. 2b) decreased to (370 ± 10 nm) at 800 °C (Fig. 2c) while the particle size increased with temperature because of further crystallization and coalescence of the grains. In addition, the EDX analysis (Fig. 2d) further confirmed that $CdTiO_3$ nanofibers were composed of Cd, Ti and O, no other impurity element is detected, indicating the final product is free of impurity. The atomic ratio of Cd to Ti is about 1:1 which was close to the theoretical value.

TEM was used to investigate the microstructure of the sample in more detail. Fig. 3a shows the agglomerated nanoparticle on nanofibers. The SAED pattern (Inset Fig. 3a); composed of some bright points and rings which supports the polycrystalline nature of the nanofibers. The FFT micrograph illustrated the parallel crystalline planes which confirms high

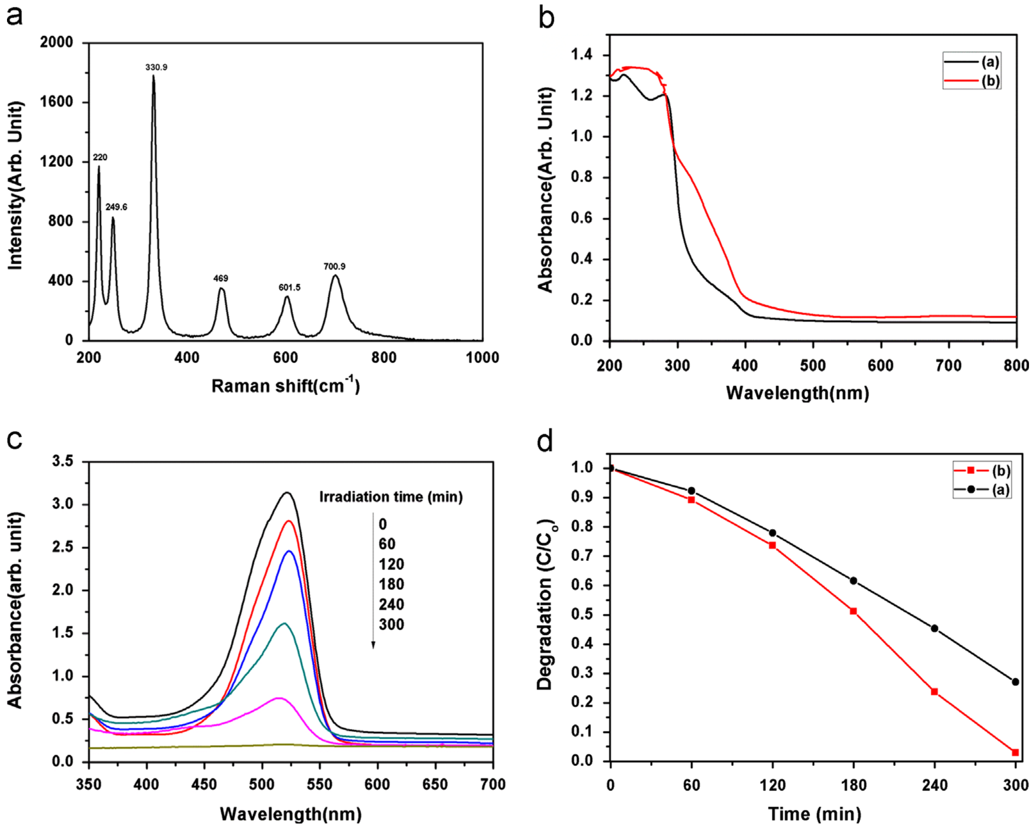

Fig. 4. (A) Raman spectrum of $CdTiO_3$ nanofibers calcined at 800 °C. (B) UV–vis DRS spectra of $CdTiO_3$ nanofibers calcined at (a) 600 °C and (b) 800 °C. (C) Absorption spectra of RB solutions in the presence of $CdTiO_3$ nanofibers calcined at 800 °C under UV light at different periods of time. (D) Photocatalytic activity of $CdTiO_3$ nanofibers calcined at (a) 600 °C and (b) 800 °C for R6G degradation.

crystallinity of the sample (Inset Fig. 3a). The TGA thermograms of PVAc/$Cd(NO_3)_2 \cdot 6H_2O$/TiP composite were shown in Fig. 3b. As pointed out by the TGA, pure PVAc fibers started to decompose up to 60% at 450 °C because their decomposition temperature was about 150 °C, and completely at above 500 °C. On the first derivative curve, a main exothermic peak was observed at 337 °C, suggesting the thermal events related to the decomposition of titanium tetra-isopropoxide and cadmium nitrates along with the degradation of PVAc by dehydration on the polymer side chain, which was confirmed by a dramatic weight loss in TG curve at the corresponding temperature range (200–500 °C).

Fig. 4a shows the Raman spectrum of the synthesized $CdTiO_3$ nanofibers at 800 °C. Six peaks appeared around 220, 249, 330, 469, 601 and 701 cm^{-1} in the Raman shift range of 200–900 cm^{-1}. The first three peaks are sharp and peak at 330 cm^{-1} is the sharpest. While the last three peaks are wide. So, the rhombohedral symmetry of $CdTiO_3$ was again confirmed by the Raman spectra which are in accordance with those reported in the previous literatures [22,23]. The Diffuse reflection adsorption spectra (DRS) of the $CdTiO_3$ nanofibers synthesized at different temperatures was shown in Fig. 4b. The sample calcined at 800 °C showed a little stronger absorbance compared to the sample calcined at 600 °C. The increase in calcination temperature led to a marginal red shift in 490 nm absorbance band. The difference in absorbance spectra of samples at different temperature may be due to the difference in size of the particles (Quantum size effect) [24]. Band gap energy calculated from the spectra at 600 °C is 3.82 and at 800 °C is 2.81 eV. The red shift of the absorption edge towards the visible region may be beneficial for improving the photoabsorption and photocatalytic performance of $CdTiO_3$ nanofibers.

Photocatalytic decomposition of R6G dye was used to evaluate the photocatalytic activities of the synthesized $CdTiO_3$ nanofibers. It has been reported in the literature that the photocatalytic activities of catalysts depend on many factors, such as crystallinity, surface properties, absorption properties, and so on [25]. As observed in Fig. 4c, the major absorption peaks of R6G around 521 nm diminished gradually under UV light irradiation in the presence of $CdTiO_3$ nanofibers calcined at 800 °C. Furthermore, in the comparative experiments, nanofibers calcined at 800 °C showed the higher photocatalytic activities than sample calcined to 600 °C (Fig. 4d). This increase in photocatalytic activity may be due to the high degree of crystallinity and red shifts to longer wavelengths of the sample calcined at high temperature [26]. The degradation efficiency of R6G was about 73% and 97% for the sample synthesized at 600 °C and 800 °C respectively.

4. Conclusions

$CdTiO_3$ nanofibers were successfully synthesized by the sol–gel elecrtrospinning technique and were assayed for photocatalytic activity. $CdTiO_3$ nanofibers calcined at 800 °C were found to exhibit higher photocatalytic activities than the sample calcined at 600 °C because of the higher crystallinity and red shifts to longer wavelengths of the sample. The present investigation clearly indicates the potential use of electrospun $CdTiO_3$ nanofibers for the removal of pollutants and noxious wastes.

Acknowledgment

This work was supported by the Industrial Strategic Technology Development Program, 10041994, funded by the Ministry of Knowledge Economy (MKE, Korea)

References

[1] P. Borker, A.V. Salker, Photocatalytic degradation of textile azo dye over $Ce_{1-x}Sn_xO_2$ series, Materials Science and Engineering: B 133 (2006) 55–60.

[2] J. Sun, X. Wang, J. Sun, R. Sun, S. Sun, L. Qiao, Photocatalytic degradation and kinetics of Orange G using nano-sized Sn(IV)/TiO_2/AC photocatalyst, Journal of Molecular Catalysis A: Chemical 260 (2006) 241–246.

[3] M. Saquiba, M.A. Tariqa, M. Faisala, M. Muneer, Photocatalytic degradation of two selected dye derivatives in aqueous suspensions of titanium dioxide, Desalination 219 (2008) 301–311.

[4] J. Madhavan, P. Maruthamuthu, S. Murugesan, S. Anandan, Kinetic studies on visible light-assisted degradation of acid red 88 in presence of metal-ion coupled oxone reagent, Applied Catalysis B: Environmental 83 (2008) 8–14.

[5] K. Nakata, A. Fujishima, TiO_2 photocatalysis: design and applications, Journal of Photochemistry and Photobiology C: Photochemistry Reviews 13 (2012) 169–189.

[6] J. Zeng, M.D. Xin, K.W. Li, H. Wang, H. Yan, W.J. Zhang, Transformation process and photocatalytic activities of hydrothermally synthesized Zn_2SnO_4 nanocrystals, Journal of Physical Chemistry C112 (2008) 4159–4167.

[7] Z. Zhu, J. Du, J. Li, Y. Zhang, D. Liu, An EDTA-assisted hydrothermal synthesis of $BiVO_4$ hollow microspheres and their evolution into nanocages, Ceramics International 38 (2012) 4827–4834.

[8] M. Zhang, C. Shao, P. Zhang, C. Su, X. Zhang, P. Liang, Y. Sun, Y. Liu, Bi_2MoO_6 microtubes: controlled fabrication by using electrospun polyacrylonitrile microfibers as template and their enhanced visible light photocatalytic activity, Journal of Hazardous Materials 225–226 (2012) 155–163.

[9] T. Yan, L. Li, W. Tong, J. Zheng, Y. Wang, G. Li, $CdWO_4$ polymorphs: selective preparation, electronic structures, and photocatalytic activities, Journal of Solid State Chemistry 184 (2011) 357–364.

[10] H. Wang, X.X. Zhang, A.P. Huang, H.Y. Xu, M.K. Zhu, B. Wang, H. Yan, M. Yoshimura, A new phase of cadmium titanate by hydrothermal method, Journal of Crystal Growth 246 (2002) 150.

[11] A.R. Phani, S. Santucci, Microwave irradiation as an alternative source for conventional annealing: a study of pure TiO_2, $NiTiO_3$, $CdTiO_3$ thin films by a sol–gel process for electronic applications, Journal of Physics: Condensed Matter 18 (2006) 6965.

[12] Shahzad Abu Bakar, S.T. Hussain, M. Mazhar, $CdTiO_3$ thin films from an octa-nuclear bimetallic single source precursor by aerosol assisted chemical vapor deposition (AACVD), New Journal of Chemistry 36 (2012) 1844–1851.

[13] A.R. Phani, M. Passacantando, S. Santucci, Synthesis and characterization of cadmium titanium oxide powders by sol–gel technique, Journal of Material Science 35 (2000) 5295–5299.

[14] Z. Imran, S.S. Batool, H. Jamil, M. Usman, M. Israr-Qadir, S.H. Shah, S. Jamil-Rana, M.A. Rafiq, M.M. Hasan, M. Willander, Excellent humidity sensing properties of cadmium titanate nanofibers, Ceramics International 39 (2013) 457–462.

[15] M.E. de Anda Reyes, G.T. Delgado, R.C. Pérez, J.M. Marín, O.Z. Ángel, Optimization of the photocatalytic activity of CdO+CdTiO3 coupled oxide thin film obtained by sol–gel technique, Journal Of Photochemistry and Photobiology A: Chemistry 228 (2012) 22–27.

[16] S.A. Maye´n-Herna´ndez, J. Santos-Cruz, G. Torres-Delgado, R. Castanedo-Pe´rez, J. Ma´rquez-Mari´n, J.G. Mendoza-Alvarez, O. Zelaya-Angel, Surface & Coatings Technology 200 (2006) 3567–3572.

[17] M.R. Mohammadi, D.J. Fray, Low-temperature perovskite-type cadmium titanate thin films derived from a simple particulate sol–gel process, Acta Materialia 57 (2009) 1049–1059.

[18] Y.C. Zhang, G.L. Wang, X.Y. Hu, W.D. Zhou, Low-temperature solid-phase synthesis of pure $CdTiO_3$ submicrocrystals using CdO_2 nanoparticles as a precursor, Journal of Crystal Growth 285 (2005) 600–605.

[19] H. Wang, X.X. Zhang, A. Huang, H.Y. Xu, M.K. Zhu, B. Wang, H. Yan, M. Yoshimura, A new phase of cadmium titanate by hydrothermal method, Journal of Crystal Growth 246 (2002) 150–154.

[20] J.G. Yu, H.T. Guo, S.A. Davis, S. Mann, Fabrication of hollow inorganic microspheres by chemically induced self-transformation, Advanced Functional Materials 16 (2006) 2035–2041.

[21] Y. Zhang, G. Li, Y. Wu, Y. Luo, L. Zhang, The formation of mesoporous TiO_2 spheres via a facile chemical process, Journal of Physical Chemistry:B 109 (2005) 5478–5481.

[22] D. Bersani, P.P. Lottici, M. Canali, A. Montenero, G. Gnappi, Sol–Gel Preparation and Raman Characterization of $CdTiO_3$, Journal of Sol–Gel Science Technology 8 (1997) 337–342.

[23] A. Montenero, M. Canali, G. Gnappi, D. Bersani, P.P. Lottici, P. Nunziante, E. Traversa, Structural and electrical properties of sol–gel-processed $CdTiO_3$ powders and films, Applied Organometallic Chemistry 11 (1997) 137–146.

[24] D.L. Liao, C.A. Badour, B.Q. Liao, Preparation of nanosized TiO_2/ZnO composite catalyst and its photocatalytic activity for degradation of methyl orange, Journal of Photochemistry and Photobiology A: Chemistry 194 (2008) 11–19.

[25] M. Saif, M.S.A. Abdel-Mottaleb, Titanium dioxide nanomaterial doped with trivalent lanthanide ions of Tb, Eu and Sm: preparation, characterization and potential applications, Inorganic Chimica Acta 360 (2007) 2863–2874.

[26] Dong Suk Kim, Seung-Yeop Kwak, The hydrothermal synthesis of mesoporous TiO_2 with high crystallinity, thermal stability, large surface area, and enhanced photocatalytic activity, Applied Catalysis A: General 323 (2007) 110–118.